Journal of ELECTRONIC MATERIALS, Vol. 48, No. 11, 2019
https://doi.org/10.1007/s11664-019-07502-1

Low-Temperature Sintering and Enhanced Dielectric Properties of $BaZr_{0.2}Ti_{0.8}O_3$-Based Y5V Ceramics with Li_2CO_3 to Reduce the Sintering Temperature

YANJUN WANG,[1] RONG MA,[1,2] XIAOTING ZHANG,[1] LILI ZHAO,[3] and BIN CUI[1,4]

1.—Key Laboratory of Synthetic and Natural Functional Molecule of Ministry of Education, Shaanxi Key Laboratory of Physico-Inorganic Chemistry, College of Chemistry and Materials Science, Northwest University, Xi'an 710127, People's Republic of China. 2.—Faculty of Chemistry and Chemical Engineering, Baoji University of Arts and Sciences, 1 Hi-Tech Avenue, Baoji 721013, Shaanxi, People's Republic of China. 3.—School of Information Science and Technology, Northwest University, Xi'an 710127, People's Republic of China. 4.—e-mail: cuibin@nwu.edu.cn

We synthesized $BaTi_{0.8}Zr_{0.2}O_3$ (BZT)-based powders using the sol–gel method, and introduced Li_2CO_3 with a low melting point (723°C) as a source of the liquid phase to reduce the sintering temperature (T_s) and improve the dielectric properties of the BZT-based ceramics. The x-ray powder diffractometer patterns exhibited a perovskite structure in all samples. The scanning electron microscope images revealed that the sinterability of the BZT-based ceramics was improved by adding an appropriate amount (3.0 wt.%) of Li_2CO_3; T_s decreased from 1280°C to 1100°C. The BZT-based ceramics sintered at 1100°C with 3.0 wt.% Li_2CO_3 met the Y5V requirements, with good electrical properties: ε_{max} = 17987, ε_r = 15950, and tan δ = 0.02. The results indicated that Li_2CO_3 can improve the dielectric properties and reduce the T_s of BZT-based ceramics. Our method therefore represents a less expensive approach for developing materials suitable for use in multilayer capacitors.

Key words: Sintering temperature, density, dielectric properties, sol–gel method

INTRODUCTION

Multilayer ceramic capacitors (MLCCs) that meet the Y5V specifications of the Electronic Industries Alliance standard are among the most used and highly developed ceramic capacitors in the world. In the Y5V specification, their dielectric capacitance (ε) must be $-82\% \le [\varepsilon_{r\ (T)} - \varepsilon_{r\ (25°C)}]/\varepsilon_{r\ (25°C)} \le 22\%$ at temperatures ranging from −30°C to 85°C.[1,2] Y5V-type $BaTiO_3$ (BTO)-based ceramics with high dielectric constants and high dielectric reliability are widely used in MLCCs.[3] Currently, BTO-based powders are prepared using conventional solid-phase methods or wet chemical methods, and high-dielectric ceramics are prepared from these materials using solid-phase doping technologies.[4] These include BTO-based ceramics with a maximum dielectric constant (ε_{max}) of 15,000 and a grain size larger than 10 μm.[5] CaO and ZrO_2 are added to BTO-based ceramics to produce good dielectric properties and a grain size of 7.5 μm.[6]

Unfortunately, the solid-phase method does not achieve uniform mixing of the doping components, and the average particle size of the prepared ceramics is large, making them unsuitable for use in high-capacity MLCCs with thin layers.[6] Researchers have instead used liquid-phase methods to produce fine-grained ceramics or monodispersed nanopowders. BTO-based ceramics have been prepared from these materials using a precipitation method, and the ε_{max} of the prepared ceramics was less than 6000.[7,8] Wang et al.[9] constructed

(Received March 12, 2019; accepted July 30, 2019; published online August 13, 2019)

fine-grained $BaZ_{r0.1}Ti_{0.9}O_3$ ceramics using a wet chemical approach and achieved an ε_{max} of 5800. Nevertheless, the precipitation process requires multiple washings, which can lead to segregation of the components and deterioration of the dielectric constant.[8,9]

BZT-based Y5V ceramics with a dielectric constant of 20,000 have been prepared by our research team using the sol–gel method, but the T_s was high (1280°C).[10] Thus, it was necessary to reduce the sintering temperature (T_s) and improve the performance of the BZT-based Y5V ceramics to make them more suitable for use in MLCCs. Three main approaches have been used to achieve low-temperature sintering of ceramics: adding sintering aids, synthesizing high-activity powders, and improving the sintering process. A lead-free $(1 - x)$ $Na_{0.5}Bi_{0.5}TiO_3$-x BTO solid solution was prepared using the sol–gel auto-combustion technique and sintered by means of microwave sintering.[11,12] However, the equipment used in this approach is expensive and not widely available, which has hindered the development of microwave sintering technology. The addition of sintering aids can effectively reduce the T_s of ceramics.[13] For example, adding Bi_2O_3-B_2O_3-SiO_2[14] and ZnO-B_2O_3-SiO_2[15] glass to BTO material can reduce the T_s to 850°C, but unfortunately, this deteriorates the permittivity of the ceramics below 1000. Sun et al.[16] prepared BZT ceramics sintered at 1250°C by means of solid-state doping with CuO, and created ceramics with a dielectric constant of 8000. Li_2CO_3 has a lower melting point (723°C), and can effectively reduce T_s. In addition, the Li^+ cations (0.076-nm diameter) can replace Ti^{4+} (0.0605-nm diameter) in BTO-based ceramics, and this can improve the material's dielectric properties.[17] Hee and Hyuk[18] prepared (Ba, Sr)TiO_3 ceramics doped with Li_2CO_3 using a solid-phase method and decreased the T_s of (Ba, Sr)TiO_3 from 1350°C to 900°C, but the dielectric properties did not meet the Y5V standard.

A high-activity powder was fabricated using a sol–gel method, permitting the production of Y5V ceramic materials with a high dielectric constant, but the T_s was high. The low melting point of Li_2CO_3 was used to keep this material at the grain boundary of BZT-based ceramics, where it formed a liquid phase that promoted sintering of BZT-based ceramics, and another advantage is that Li^+ compounds can be modified to improve the dielectric properties of ceramics, making this an effective strategy for the preparation of ceramics with a high dielectric constant and low T_s. In the present study, we therefore prepared BZT-based powders using the sol–gel method to obtain high-performance powders, and investigated the effects of the amount of Li_2CO_3 on the phase structure, microstructure, and dielectric properties of the ceramics produced from the powder. Our results provide a theoretical foundation for improving the dielectric properties and reducing the T_s of BZT-based ceramic materials.

EXPERIMENTAL PROCEDURES

We used the following analytical-grade raw materials: $Ba(Ac)_2$ (99.0%), $Zr(NO_3)_4{\cdot}5H_2O$ (99.5%), $Ce(NO_3)_3{\cdot}6H_2O$ (99.0%), $Zn(Ac)_2{\cdot}2H_2O$ (99.0%), $Cu(Ac)_2{\cdot}H_2O$ (99.5%), $Mn(Ac)_2{\cdot}4H_2O$ (99.5%), Li_2CO_3 (97.0%), and $Ti(OC_4H_9)_4$ (99.0%). The BZT-based powders were synthesized using the sol–gel approach.[10] The main component was BZT, with 0.3 wt.% MnO_2, 0.3 wt.% CeO_2, 1.5 wt.% ZnO, and 1.0 wt.% CuO added to improve the dielectric properties of the ceramics. We prepared a series of BZT-based ceramics with Li_2CO_3 added: $BZTL_x$, where x = 0 wt.%, 1.0 wt.%, 2.0 wt.%, 3.0 wt.%, and 4.0 wt.% Li_2CO_3. Li_2CO_3 was mixed with calcinated BZT powders. The powders were pressed into pellets approximately 7 mm in diameter and then calcined at 1100°C for 4 h at a heating rate of 4°C/min. The surfaces of the pellets were polished, and electrodes were prepared with high-purity silver paint and dried at 750°C for 15 min.

We used x-ray diffraction (XRD, D8 Advance, Bruker, Germany) to examine the phase structure of the powders and ceramics. We cleaned the ceramics by means of 5 min of ultrasonication in water to remove surface pollutants. We then observed the microstructure of the natural surface of the ceramics using a scanning electron microscope (SEM; TM 3000, JEOL, Tokyo, Japan). We characterized the morphology of the particles using field-emission transmission electron microscopy (FE-TEM; Tecnai G2 F20S-TWIN, FEI, Hillsboro, OR, USA). We measured the P-E hysteresis loops using a ferroelectric tester (Model 609B, Radiant Technology, Seattle, WA, USA). We measured the dielectric properties of the ceramics using an LCR tester (Model HP4284A, Hewlett-Packard, Palo Alto, CA, USA) with a high- and low-temperature test chamber.

RESULTS AND DISCUSSION

Figure 1 shows the morphology and size distribution of the particles in the BZT-based powders. The particles in the BZT-based powders were spherical, with a mean particle size of 30 nm and grains ranging from 23 nm to 38 nm in size (Fig. 1b). We observed agglomeration, which suggests high activity of the powders prepared by the sol–gel method.

Figure 2 shows the phase composition of the $BZTL_x$ ceramics. Figure 2a shows a perovskite phase structure without a secondary phase at Li_2CO_3 contents less than 3.0 wt.%, indicating that the Li^+ dissolved completely in the BZT lattice to form a solid solution. However, at x = 4.0 wt.%, a $BaLi_2Ti_6O_{14}$ (JCPDS 54-0936) phase appeared. This occurred because Li^+ had exceeded the solid solution limit and gathered at the grain boundary to form the second phase.[19] Figure 2b shows the enlarged XRD patterns from 2θ = 44°–46° for the $BZTL_x$ ceramics. The split of the 002/200 peak, which represents tetragonality, was consistent with the c/a value calculated from the lattice parameters,

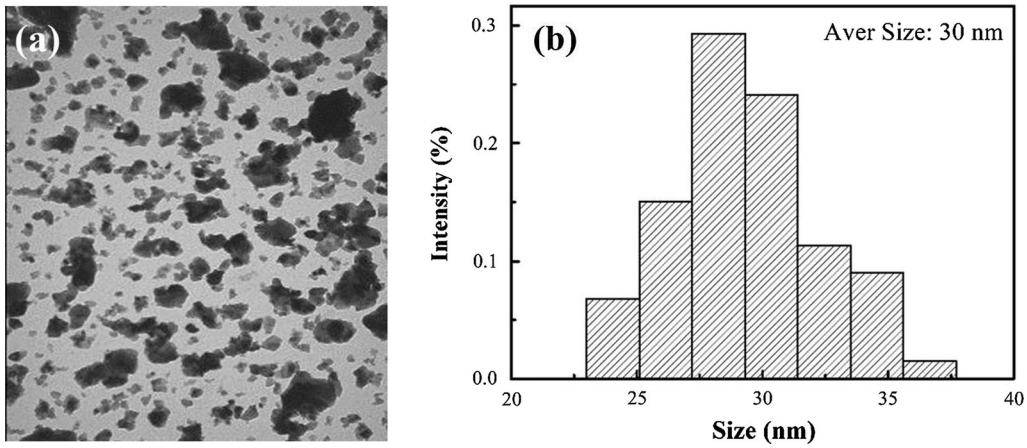

Fig. 1. TEM images (a) and grain-size distributions for BZT-based powder (900°C/2 h) (b).

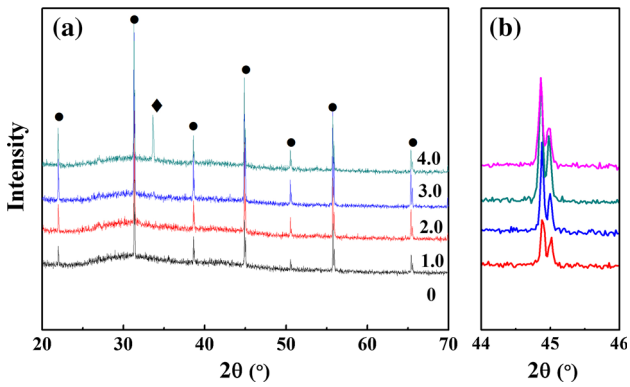

Fig. 2. XRD patterns of the $BZTL_x$ ceramics with Li_2CO_3 sintered at 1100°C: (a) XRD patterns with Li_2CO_3 addition ranging from 0 wt.% to 4.0 wt.% Li_2CO_3, (b) enlarged XRD patterns for 2θ between 44° and 46°.

with values of 2.4388 at 0 wt.%, 2.4453 at 1.0 wt.%, 2.4468 at 2.0 wt.%, and 2.4486 at 3.0 wt.% and 4.0 wt.% (Table I). This indicates that the tetragonal phase content in the ceramic increased while x remained less than 3.0. The position of diffraction peak for the ceramic sample gradually shifted to a lower value with increasing x below 3.0 wt.%. These shifts demonstrate that the larger-radius Li^+ (0.076 nm) entered the B-site to replace the smaller-radius Ti^{4+} (0.0605 nm).[20]

To obtain further insights into the compositional changes, we analyzed the changes in surface chemistry of the $BZTL_x$ pellets at the grain boundaries for C 1*s*, Ti 2*p*, Zr 3*d*, O 1*s*, and Li 1*s*. Figure 3 shows the x-ray photoelectron spectroscopy (XPS) spectra for the $BZTL_3$ and $BZTL_4$ pellets. We quantified the XPS results using the following equation:

$$C = I/S \quad (1)$$

where I is the area of the Li 1*s* and S is the sensitivity factor. It is apparent that the Li^+ content of $BZTL_3$ is much lower than that of $BZTL_4$ because Li^+ exceeds the solid solution limit in $BZTL_4$ and is distributed at the grain boundary.[19] These results are consistent with the XRD results, and confirm that Li^+ enters the lattice during the later sintering stages, and can improve the dielectric properties of the ceramics at less than 3.0 wt.% Li_2CO_3.

Figure 4 shows the surface morphology of the $BZTL_x$ ceramics. The pure BZT ceramics in Fig. 4a show a porous microstructure. The grain size first increased and then slightly decreased with increasing x. The average particle size in the ceramics was 6.7 μm, 7.6 μm, 8.5 μm, and 8.1 μm, respectively, for x = 1.0, 2.0, 3.0, and 4.0. As x increased from 1.0 to 3.0, the densification of the ceramics improved greatly, and the porosity of the ceramics compared with the sample without Li_2CO_3. This is probably because a liquid phase formed due to the low melting point of Li_2CO_3 (723°C), and the liquid will promote grain growth and densification by facilitating the dissolution and migration of the chemical species.[21] Li^+ replaces high-valence Zr^{4+} or Ti^{4+} at B-sites during later stages of the sintering process, leading to the development of an oxygen vacancy to maintain the charge balance. This is also beneficial for the transport of species during the sintering process, thereby promoting the growth and densification of the ceramic grains.[22] However, at 4.0 wt.%, more pores develop between the ceramic grains and more "closed pores" form inside the ceramics due to the increased liquid phase, which leads to abnormal growth of the particles and the formation of more CO_2.[23]

The density of the ceramics increased from 4.48 g/cm^3 with no Li_2CO_3 to 5.34 g/cm^3 at 1.0 wt.%, then to 5.58 g/cm^3, 6.72 g/cm^3, and 5.62 g/cm^3 at 2.0 wt.%, 3.0 wt.%, and 4.0 wt.%, respectively. The corresponding relative densities were 88%, 92%, 94%, and 93%. The maximum relative density of 94% at 3.0 wt.% shows that the introduction of Li_2CO_3 can effectively increase the relative density of the ceramics. The decrease in the relative density

Table I. Summary of the parameters of the $BaTi_{0.8}Zr_{0.2}O_3$-based ceramic materials

Li_2CO_3 (wt.%)	a (Å)	c (Å)	c/a	Density (g/cm^3)	P_r (μC/cm^2)	P_{max} (μC/cm)	E_c (kV/m)
0	5.7253	13.9635	2.4388	4.48	0.48	4.57	2.06
1	5.7189	13.9844	2.4453	5.34	1.54	12.15	2.92
2	5.7105	13.9726	2.4468	5.58	24.84	30.01	30.4
3	5.7013	13.9746	2.4486	5.72	27.29	33.15	32.0
4	5.7102	13.9820	2.4486	5.62	7.74	14.28	13.0

P_r, remanent polarization; P_{max}, maximum polarization; E_c, electrical coercivity.

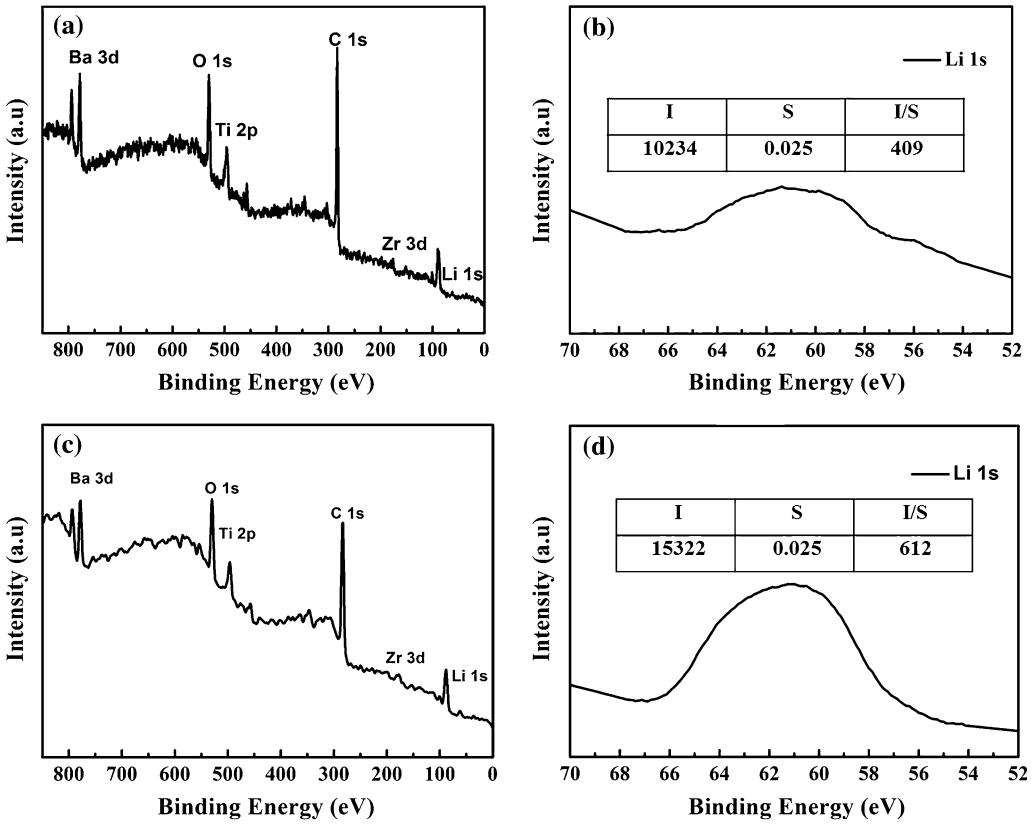

Fig. 3. XPS spectra and the expanded spectra of Li 1*s* for $BZTL_3$ ceramics (a, b) and $BZTL_4$ ceramics (c, d).

at 4.0 wt.% results from the fact that more of the liquid phase is produced during the later sintering stages, and more CO_2 is evolved because of decomposition of Li_2CO_3, resulting in increased porosity.[21,23] On the other hand, the closed pores between the grains increase as the ceramic particle size increases at Li_2CO_3 of 4.0 wt.%, which can led to the decreased density.[24]

Figure 5 shows the temperature dependence of the dielectric properties. Table II summarizes the main properties of the $BZTL_x$ ceramics. The dielectric constants of the samples at room temperature (ε_r) first increased and then decreased with increasing Li_2CO_3, but the Curie temperature (T_c) decreased. This may be caused by Li^+ ions entering B-sites in the lattice of ABO_3, which affects the stability of the octahedral phase.[25]

The change in the dielectric constant with increasing Li_2CO_3 is consistent with the changes in density and grain size. The 3.0 wt.% $BZTL_x$ ceramics sintered at 1100°C exhibited good electrical properties: ε_{max} = 17987, ε_r = 15950, and tan δ = 0.02. It is obvious that generation of the Li_2CO_3 liquid phase facilitates mass transfer processes, and that sintering of the ceramics was promoted by increasing the Li_2CO_3 content, thereby increasing the dielectric constant of the ceramics with increasing average particle size and density.[26] However, the dielectric constant decreased with further increases in the Li_2CO_3 content. On the one hand,

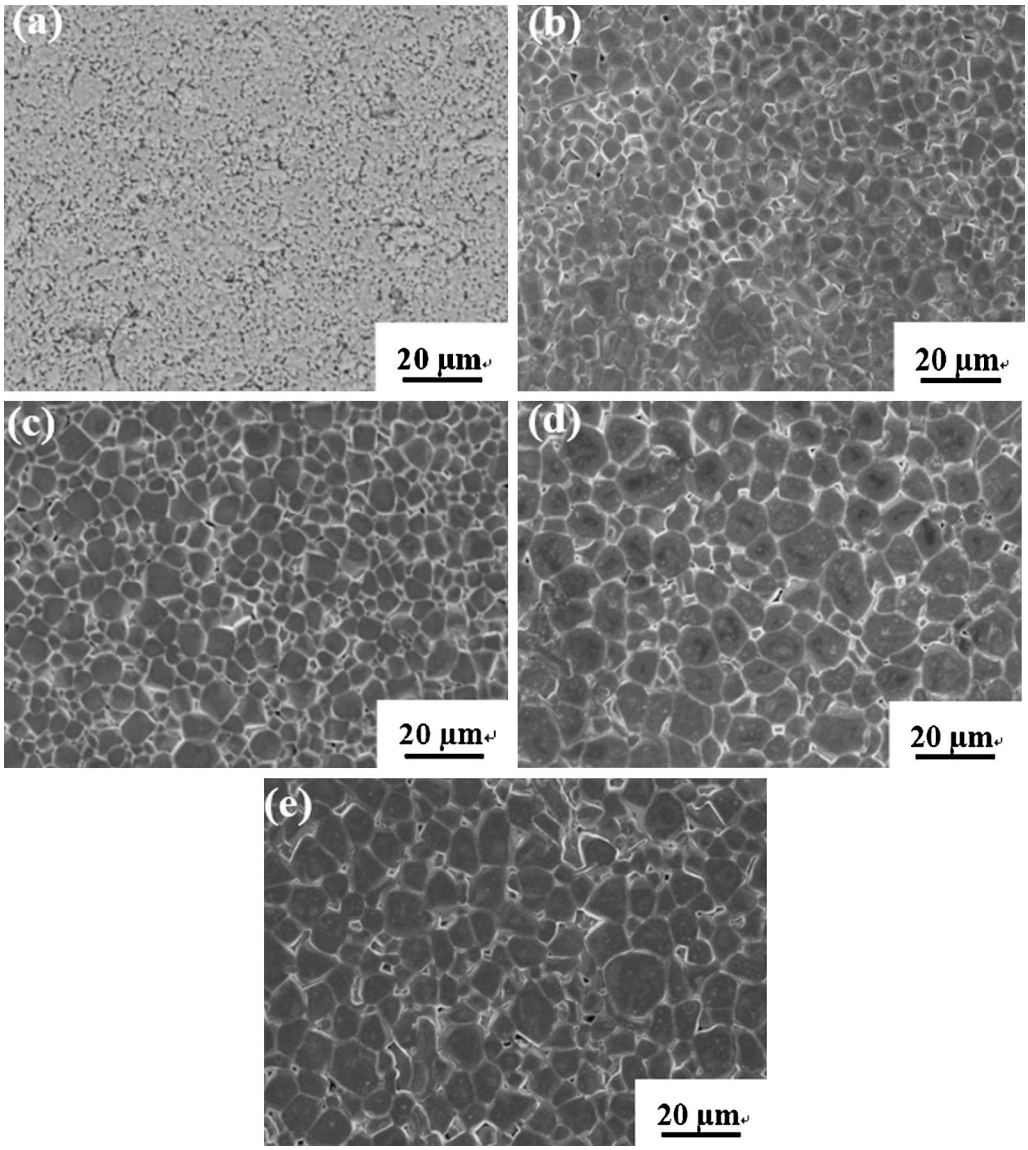

Fig. 4. SEM images of the $BZTL_x$ ceramics sintered at 1100°C for 4 h: (a) no added Li_2CO_3; (b) 1.0 wt.% Li_2CO_3; (c) 2.0 wt.% Li_2CO_3; (d) 3.0 wt.% Li_2CO_3; (e) 4.0 wt.% Li_2CO_3.

the increase of the dielectric constant of the ceramics results from the pinning effect of the domain walls and the increased compaction of the ceramics. There are more 90° domains in large ceramic grains, which could help the domain walls flip more easily.[27] On the other hand, excess Li_2CO_3 increases the porosity of the ceramics and leads to the formation of a second phase ($BaLi_2Ti_6O_{14}$) at 4.0 wt.%, thereby diluting the ferroelectric phase and leading to deterioration of the dielectric properties.[28]

Figure 6 shows the phase composition of the $BZTL_3$ ceramics after sintering at different T_s. It appears that T_s had no significant effect on the phase structure of the ceramics and that all samples were perovskite-phase structures. This may be because Li^+ was solid-solved into the BZT lattice, and no second phase was generated at 3.0 wt.% or less.[29]

Figure 7 shows SEM images of the ceramics sintered at various T_s. The grain size of the $BZTL_3$ ceramics grew obviously, and the number of pores increased as the sintering temperature increased. The grain sizes after sintering at 1050°C, 1100°C, and 1150°C were 5.8 μm, 7.6 μm, and 7.9 μm, respectively. The increased grain size was conducive to mass transfers in the material, as the increased T_s can accelerate material transfers and increase mobility at the grain boundary, leading to coarsening of the ceramic grains, usually accompanied by the formation of polyhedrons with more distinct edges and corners, which leads to growth of the ceramic grains. When the sintering temperature was 1150°C, the ceramic grains grew abnormally

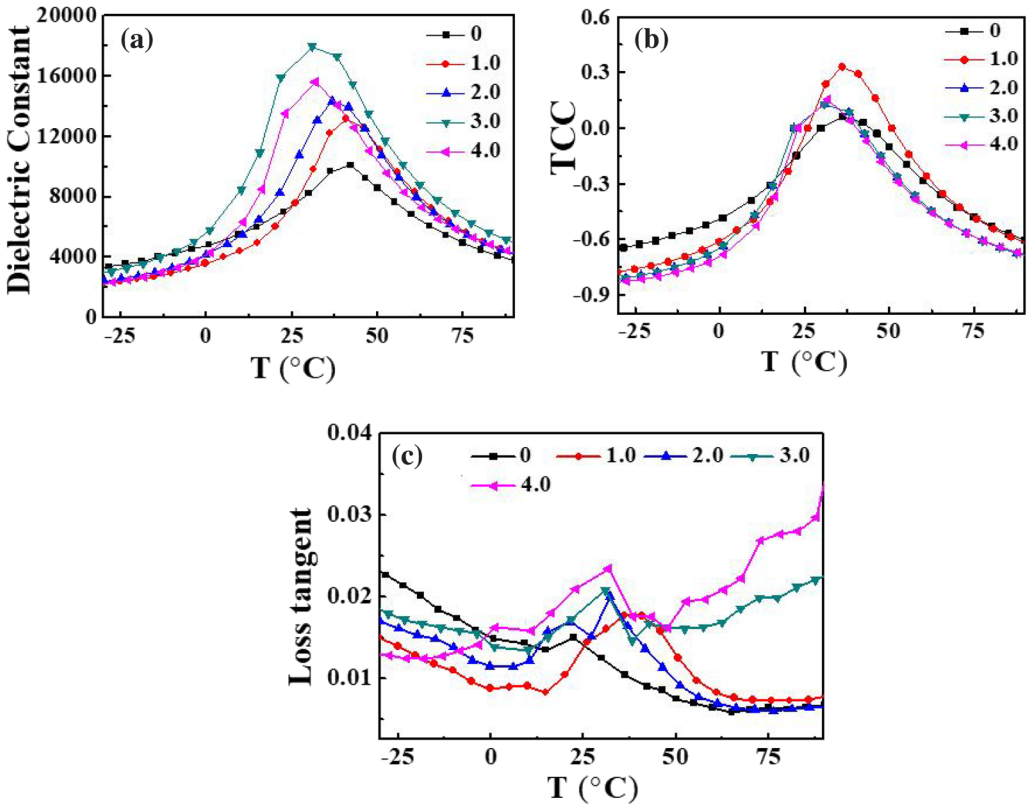

Fig. 5. Temperature dependence of the (a) dielectric constant, (b) temperature capacitance characteristic (TCC), and (c) dielectric loss for BZT-based ceramics with Li_2CO_3 added at 0–4.0 wt.% and sintered at 1100°C.

Table II. Main dielectric properties of the BZT ceramics with Li_2CO_3 added and sintered at 1100°C for 4 h

				TCC (%)		
Li_2CO_3 (wt.%)	**tan δ (25°C)**	**ε_r**	**T_C**	**−30°C**	**T_c**	**85°C**
0	0.01	8104	36.2	−58.0	20.0	−57.04
1.0	0.01	7594	38.8	−70.0	34.0	−62.90
2.0	0.01	10,785	36.8	−77.0	0.062	−69.05
3.0	0.02	15,950	30.8	−81.0	0.38	−64.53
4.0	0.04	13,517	30.2	−82.0	4.30	−64.27

ε_r, dielectric constant at room temperature (25°C); T_c, Curie temperature; TCC, temperature capacitance characteristic.

and there were more and larger pores, which would decrease the dielectric constant.[30] Therefore, choosing appropriate T_s is particularly critical for producing the optimal size and dielectric properties of these ceramics.

Figure 8 shows the effect of T_s on the dielectric properties of the $BZTL_3$ ceramics. Table III summarizes their main properties. ε_r was 8122, 15950, and 14844 at T_s of 1050°C, 1100°C, and 1150°C, respectively. That is, ε_r of the ceramics first increased and then decreased, and T_c shifted to a lower temperature. The dielectric properties of the ceramics are closely related to their phase structure, microstructure, and grain size.[21] After sintering at 1050°C, the ceramic grains had a uniform size, and there were fewer and smaller pores between the grains. When T_s increased to 1100°C, the grain size of the ceramics increased and became more uniform, which helps movement of domain walls and improves the ceramic's dielectric properties. However, when the temperature increased to 1150°C, the ceramic grains grew abnormally, resulting in the appearance of more pores between the grains, thereby deteriorating the dielectric properties.[23] Figure 8a and Table III show that the ε_r of the $BZTL_3$ ceramics sintered at 1100°C was 15,950. The corresponding dielectric loss was 0.02, and temperature capacitance characteristic (TCC) met the Y5V standard.

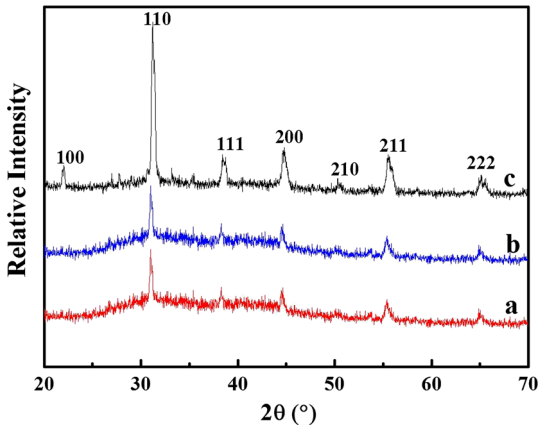

Fig. 6. XRD patterns for BZT-based ceramics with 3.0 wt.% Li_2CO_3 sintered at different temperatures: (a) 1050°C; (b) 1100°C; (c) 1150°C.

CONCLUSIONS

In this study, we synthesized BZT-based Y5V ceramics with the addition of Li_2CO_3 and characterized their properties. First, we prepared BZT-based powders using the sol–gel approach, and then introduced Li_2CO_3 with a low melting point (723°C) to reduce T_s and improve the dielectric properties of the BZT-based ceramics. We reduced the T_s of the BZT-based ceramics from 1280°C to 1100°C by adding Li_2CO_3. The dielectric constant of the BZT-based ceramics first increased and then decreased with increasing Li_2CO_3 addition when the powder was sintered at 1100°C. The ε_r of the BZT-based ceramics was 15,950 at 3.0 wt.% Li_2CO_3, with an average grain size of 7.6 μm and a dielectric loss of 0.02. These results indicated that Li_2CO_3 addition

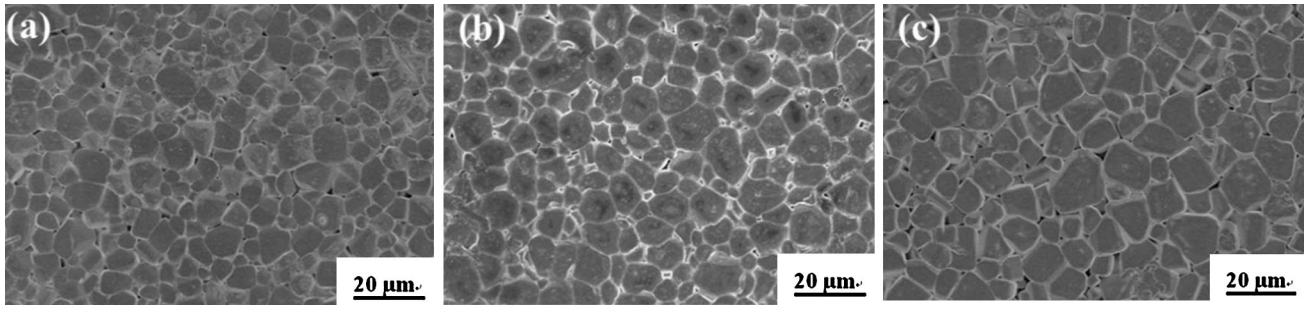

Fig. 7. SEM patterns of the $BZTL_3$ ceramics sintered at different temperatures: (a) 1050°C; (b) 1100°C; and (c) 1150°C.

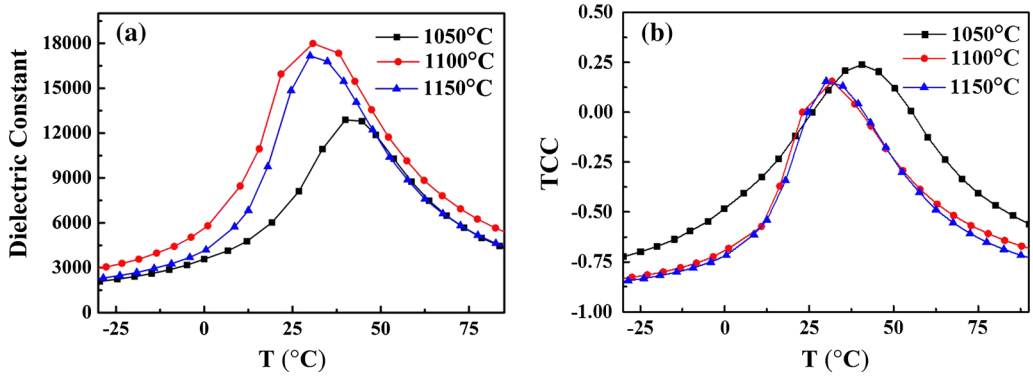

Fig. 8. Temperature dependence of (a) the room-temperature dielectric constant (ε_r) and (b) the temperature capacitance characteristic (TCC) for $BZTL_3$ samples and then after being sintered at different temperatures.

Table III. Main properties of the $BZTL_3$ and then after being sintered at different temperatures

				TCC (%)		
Sintering temperature (°C)	**Grain size (μm)**	**tan δ (25°C)**	**ε_r**	**−30°C**	**T_C**	**85°C**
1050	4.3	0.01	8122	−74.0	34.0	−50.0
1100	7.6	0.02	15,950	−81.0	16.0	−64.5
1150	7.9	0.02	14,844	−81.0	15.5	−68.0

ε_r, dielectric constant at room temperature; T_c, Curie temperature; TCC, temperature capacitance characteristic.

can improve the dielectric properties of BZT-based ceramics sintered at low temperatures, and is a potentially inexpensive way to develop multilayer capacitors.

ACKNOWLEDGMENTS

We thank the Shaanxi Province Natural Science Foundation Research Project (Grant No. 2016JZ006), the Key Laboratory of Se-enriched Products Development and Quality Control, Ministry of Agriculture and Rural Affairs/National-Local Joint Engineering Laboratory of Se-enriched Food Development (Grant No. Se-2018B06), and the Shaanxi Light Optoelectronics Material Co., Ltd. (No. 2015610002001920) for funding our research.

REFERENCES

1. J. Qi, Z. Gui, Y.L. Wang, Q. Li, and L. Li, *J. Mater. Sci. Lett.* 21, 405 (2002).
2. X. Chou, J. Zhai, J. Sun, and X. Yao, *Ceram. Int.* 4, 911 (2008).
3. J. Hong and H. Lu, *J. Am. Ceram. Soc.* 97, 2256 (2014).
4. X. Zhang, Z. Yue, B. Peng, Z. Xie, L. Yuan, and J. Zhang, *J. Am. Ceram. Soc.* 97, 2921 (2014).
5. Y.L. Wang, L.T. Li, J.Q. Qi, and Z. Gui, *Ceram. Int.* 28, 657 (2002).
6. Y.C. Wu, J.S. Lee, H.Y. Lu, and C.L. Hu, *J. Electroceram.* 18, 13 (2007).
7. K. Miao, X. Wang, D. Hu, Y. Wang, and J. Xiao, *Ceram. Int.* 43, 9099 (2017).
8. J. Wang, S.L. Jiang, D. Jiang, J. Tian, Y. Li, and Y. Wang, *Ceram. Int.* 38, 5853 (2012).
9. Y. Wang, K. Miao, and R. Ma, *Ceram. Int.* 42, 14627 (2016).
10. Y. Wang, B. Cui, L. Zhang, Z. Hu, and Y. Wang, *Ceram. Int.* 40, 11681 (2014).
11. H.S. Mohanty, T. Dam, H. Borkar, D.K. Pradhan, K.K. Mishra, A. Kumar, B. Sahoo, P.K. Kulriya, C. Cazorla, J.F. Scott, and D.K. Pradhan, *J. Phys. Condens. Matter* 31, 075401 (2019).
12. H.S. Mohanty, A. Kumar, B. Sahoo, P.K. Kurliya, and D.K. Pradhan, *J. Mater. Sci. Mater.* 29, 6966 (2018).
13. M. Valant, D. Suvorov, R.C. Pullar, K. Sarma, and N.M. Alford, *J. Eur. Ceram. Soc.* 26, 2777 (2006).
14. J.J. Ruiz-Valdés, A.V. Gorokhovsky, and J.I. Escalante-García, *J. Eur. Ceram. Soc.* 24, 1505 (2004).
15. H.I. Hsiang, C.S. His, C.C. Huang, and S.L. Fu, *J. Alloys Compd.* 459, 307 (2008).
16. H. Sun, Y. Zhang, X. Liu, Y. Liu, and W. Chen, *Ceram. Int.* 41, 555 (2015).
17. W.G. Yang, B.P. Zhang, N. Ma, and L. Zhao, *J. Eur. Ceram. Soc.* 32, 899 (2012).
18. W.Y. Hee and K.J. Hyuk, *Integr. Ferroelectr.* 86, 59 (2006).
19. L. Zhao, B.P. Zhang, and P.F. Zhou, *J. Eur. Ceram. Soc.* 35, 533 (2015).
20. L. Zhao, B.P. Zhang, and P.F. Zhou, *J. Am. Ceram. Soc.* 97, 2164 (2014).
21. G.H. Chen and Y. Yang, *J. Mater. Sci. Mater. Electron.* 24, 1012 (2012).
22. Y.D. Hou, M.K. Zhu, H. Wang, B. Wang, C.S. Tian, and H. Yan, *J. Eur. Ceram. Soc.* 24, 3731 (2004).
23. X. Chen, X. Ruan, K. Zhao, X. He, J. Zeng, and Y. Li, *J. Alloys Compd.* 632, 103 (2015).
24. Y.D. Hou, L.M. Chang, M.K. Zhu, X.M. Song, and H. Yan, *J. Appl. Phys.* 102, 084507 (2007).
25. J. Bian and Y. Ding, *Mater. Res. Bull.* 49, 245 (2014).
26. P. Wang, Y. Li, and Y. Lu, *J. Eur. Ceram. Soc.* 31, 2005 (2011).
27. X. Liu, M. Zhu, Z. Chen, B. Fang, J. Ding, and X. Zhao, *J. Alloys Compd.* 613, 219 (2014).
28. S.K. Ye, J.Y.H. Fuh, and L. Lu, *Appl. Phys. Lett.* 100, 1153 (2012).
29. V. Buscaglia, M.T. Buscaglia, M. Viviani, L. Mitoseriu, P. Nanni, and V. Trefiletti, *J. Eur. Ceram. Soc.* 26, 2889 (2006).
30. Z. Sun, L. Li, H. Zheng, S. Yu, and D. Xu, *Ceram. Int.* 41, 12158 (2015).